

Heterogeneous & Homogeneous & Bio- & Nano-

CHEM **CAT** CHEM

CATALYSIS

Accepted Article

Title: Influence of Hydrogen Bond Donating Sites in UiO-66 Metal-Organic Framework for Highly Regioselective Methanolysis of Epoxides

Authors: Aniruddha Das, Nagaraj Anbu, Mostakim SK, Amarajothi Dhakshinamoorthy, and Shyam Biswas

This manuscript has been accepted after peer review and appears as an Accepted Article online prior to editing, proofing, and formal publication of the final Version of Record (VoR). This work is currently citable by using the Digital Object Identifier (DOI) given below. The VoR will be published online in Early View as soon as possible and may be different to this Accepted Article as a result of editing. Readers should obtain the VoR from the journal website shown below when it is published to ensure accuracy of information. The authors are responsible for the content of this Accepted Article.

To be cited as: *ChemCatChem* 10.1002/cctc.201902219

Link to VoR: <http://dx.doi.org/10.1002/cctc.201902219>

WILEY-VCH

www.chemcatchem.org



Influence of Hydrogen Bond Donating Sites in UiO-66 Metal-Organic Framework for Highly Regioselective Methanolysis of Epoxides

Aniruddha Das,^[a] Nagaraj Anbu,^[b] Mostakim SK,^[a] Amarajothi Dhakshinamoorthy^{*[b]} and Shyam Biswas^{*[a]}

[a] A. Das, M. SK, Dr. S. Biswas
Department of Chemistry
Indian Institute of Technology Guwahati, Assam 781039, India.
E-mail: sbiswas@iitg.ac.in.

[b] N. Anbu, Dr. A. Dhakshinamoorthy
School of Chemistry,
Madurai Kamaraj University, Madurai, Tamil Nadu 625021, India.
E-mail: admguru@gmail.com

Supporting information for this article is given via a link at the end of the document.

Abstract

A Zr(IV)-based UiO-66 metal-organic framework (MOF) (named **1**) was synthesized by employing 1-(aminomethyl)naphthalene-2-ol appended terephthalate linker and Zr(IV) salt via solvothermal method and subsequently characterized. Furthermore, the potential efficiency of activated (named **1'**) form of as-synthesized MOF was investigated as an organocatalyst for the ring-opening of epoxide by methanol. The catalytic performance of **1** and **1'** was studied in the methanolysis of epoxide using styrene oxide as a model substrate and the activity of **1'** was also examined with various alcohols. Under

the optimized reaction conditions, the catalytic performance of **1'** reached 96% conversion of styrene oxide to its corresponding product with 98% regioselectivity. The reusability and stability of the catalyst were proved by recycling up to four runs in the methanolysis of styrene oxide. The Lewis acidity originating from metal nodes and hydrogen bond donating (HBD) sites in the linker is distributed homogeneously throughout the framework, thus playing crucial role in the activation of epoxide with easy accessibility.

Introduction

Metal-organic frameworks (MOFs) are composed of metal ions or clusters and organic linker molecules in a highly ordered manner resulting in three-dimensional framework solids with well-defined porous structure.¹⁻³ Within a short span of time, porous MOFs have gained much attention in inorganic chemistry due to their unique properties like gas storage,⁴ gas/liquid separation,⁵ chemical sensing,⁶ molecular magnetism,⁷ drug delivery,⁸ biomedicine,⁹ optoelectronics,¹⁰ heat transformation process,¹¹ host for metal nanoparticles¹² and heterogeneous catalysis.^{11, 13-15} Particularly, Zr-based MOFs have received wider attention among other MOFs mainly due to their exceptional features like high surface area,¹⁶ high thermal and chemical stability,¹⁷ low toxicity,¹⁸ tunable pore size and shape,¹⁹ surface functionality and incorporation of a variety of functional moieties in linker molecule.²⁰ The unsaturated metal centers can act as Lewis acidic (LA) sites as well as the inclusion of Lewis acidic or Brønsted acidic (BA) functional group in linker side enhances the catalytic activity in heterogeneous catalysis.^{11, 13, 21-23}

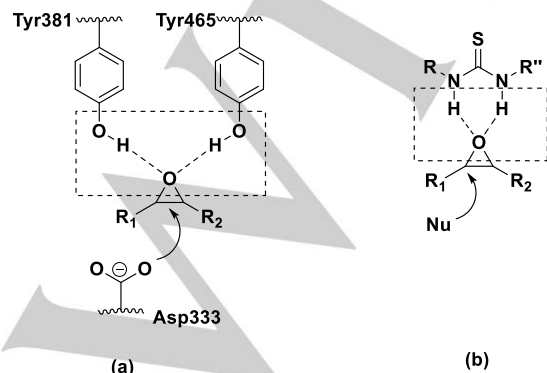
Epoxides are one of the most important intermediates in organic synthesis that can undergo nucleophilic ring-opening reactions by various nucleophiles including alcohols^{24, 25} to produce compounds like β -alkoxyalcohols, 1,2-diols and other compounds having pharmaceutical and agrochemical importance.²⁶⁻²⁸ Thus, methanol is one of the frequently used nucleophiles for the ring-opening of epoxides due to its high reactivity and importance of the resulting product.²⁹ Alcoholysis

of epoxides is a well-established chemical transformation reaction that can be achieved by various homogeneous and heterogeneous catalysts.^{24, 30-33} Alcohols having relatively poor nucleophilicity are not preferred candidates due to the production of lower yields in the ring-opening of epoxides reaction.³⁴ Hence, this type of reaction can be promoted by enhancing the electrophilicity of epoxides. Traditionally, the activation of epoxides was achieved by employing catalysts possessing either LA or BA sites or both of them.^{11, 24, 35} Historically, the methanolysis of epoxides was attained by using corrosive sulfuric acid whereas in recent times, few homogeneous catalysts based on metal complexes and different heterogeneous catalytic systems such as amberlyst-15, clays, polymers and silica were also reported.^{24, 32, 36, 37} The major problems arising during the use of homogeneous catalyst are the difficulty in the separation from the reaction mixture and inability to reuse.^{38, 39} In recent times, significant attempts have been dedicated to develop MOF based heterogeneous catalysts possessing LA metal center or BA functional groups in the linker like $-\text{SO}_3\text{H}$ and $-\text{OH}$ for the methanolysis of epoxides.^{24, 29, 34, 40-44} However, these catalytic reactions still have many drawbacks like unsatisfactory selectivity of product, robustness and recyclability of catalyst and harsh reaction conditions.^{24, 25} Hence, developing new heterogeneous catalysts to promote methanolysis of epoxide with very high regioselectivity at very high conversion of epoxide is of great interest. On other hand, it is one of the benchmark reactions to determine the nature of active sites in the as-synthesized catalysts.

The concept of double hydrogen bonding in activating the oxygen in epoxides has emerged from epoxide hydrolase

enzyme where the existence of two phenolic hydrogen atoms of two tyrosine residues are effectively involved in the activation of epoxides by establishing hydrogen bonding as shown in Scheme 1a.⁴⁵ This concept was exploited by developing a series of organocatalysts consisting of HBD sites for activation of oxygen in epoxides by introducing functional groups in an analogous fashion. Among these functional groups, urea, thiourea, catechol and related derivatives have been effectively employed as organocatalysts in homogeneous media for the activation of epoxides as shown in Scheme 1b.⁴⁶⁻⁴⁸ The development of organocatalysts with HBD motifs has become one of the powerful strategies for the activation of oxygen in epoxides by the formation of weak hydrogen bonding interactions. In one of the early examples, the rate of reaction was significantly higher with biphenylenediol as HBD type organocatalysts as compared to phenol for the addition of diethylamine to phenyl glycidyl ether. The superior activity of the former compound was attributed to the formation of two H-bonds with the oxygen atom of the electrophile.⁴⁹ Although the concept of HBD sites has been well explored in homogeneous catalysis by developing a wide range of organocatalysts, there are only limited examples of anchoring such types of catalysts in heterogeneous motifs.

One of the main objectives of this work is to obtain a UiO-66 MOF with those linkers having HBD sites for mimicking epoxide hydrolase enzyme. Herein, we report the solvothermal synthesis of a Zr(IV)-based MOF of UiO-66 topology containing 2-(((2-hydroxy naphthalene-1-yl)methyl)amino)terephthalic acid as a linker molecule consisting of HBD sites. The as-synthesized solid **1** was characterized by XRPD measurements, TGA, N₂ sorption experiment and EDX analysis. The guest free form of **1** (named **1'**) was utilized as a heterogeneous catalyst for the methanolysis reaction of epoxide. The incorporation of 1-(aminomethyl)naphthalene-2-ol moiety as side chain of linker molecule helps to activate the epoxide molecules during the methanolysis reaction. The experimental catalytic data revealed that the metal nodes inside the framework act as LA and the -OH and NH sites in the linker act as HBD sites. Both LA and HBD sites participate in the reaction. However, HBD sites influence the rate of reaction effectively in the methanolysis of styrene oxide. Furthermore, the substrate scope as well as the role of catalyst in methanolysis were checked by performing control experiments in presence of the corresponding free linker and various conventional catalysts. The stability of **1'** was ascertained by performing reusability experiments up to four cycles.



Scheme 1. Activation of oxygen in epoxide (a) epoxide hydrolase enzyme and (b) organocatalyst.

Results and Discussion

Preparation

The synthesis and characterization details of 2-(((2-hydroxy naphthalene-1-yl)methyl)amino)terephthalic acid are described in synthesis of H₂BDC-NH-CH₂-Naph-OH linker section (SI, Figures S1-S3). Different possible reactions were performed using ZrCl₄ and H₂BDC-C₁₁H₁₀NO linker in DMF solvent with various modulators (acetic acid, benzoic acid, formic acid and trifluoroacetic acid) at different temperatures.^{50, 51} A highly crystalline yellow colored precipitation of **1** was obtained upon reacting a mixture of ZrCl₄, H₂BDC-C₁₁H₁₀NO and acetic acid in 1:1:30 molar ratio in DMF at 120 °C for one day.

FT-IR study

The FT-IR spectra of free linker, **1** and **1'** were recorded (SI, Figure S4) for checking the existence of carboxylate moiety of linker molecule inside the framework of **1** and **1'**. The frequencies for asymmetric and symmetric stretching vibrations of carboxylate in free linker were found at 1701 and 1454 cm⁻¹.^{15, 18} The absorption peaks at 1576 and 1574 cm⁻¹ for **1** and **1'** were present due to the existence of asymmetric stretching vibration of carboxylate inside the framework of MOF, respectively. The characteristic peaks for symmetric stretching vibration of carboxylate were found at 1435 and 1434 cm⁻¹ for **1** and **1'**, respectively. The presence of characteristic peaks of carboxylate moiety for **1** and **1'** indicated that the linker molecules were incorporated inside the framework.^{15, 18} The shift in peak positions of symmetric and asymmetric carboxylate stretching vibrations as compared free carboxylic acid ligand is due to the binding of carboxylates with Zr(IV) ions. The peak at 1656 cm⁻¹ in as-synthesized **1** is present due to the presence of guest DMF solvent molecules which originated from the reaction medium.⁵²

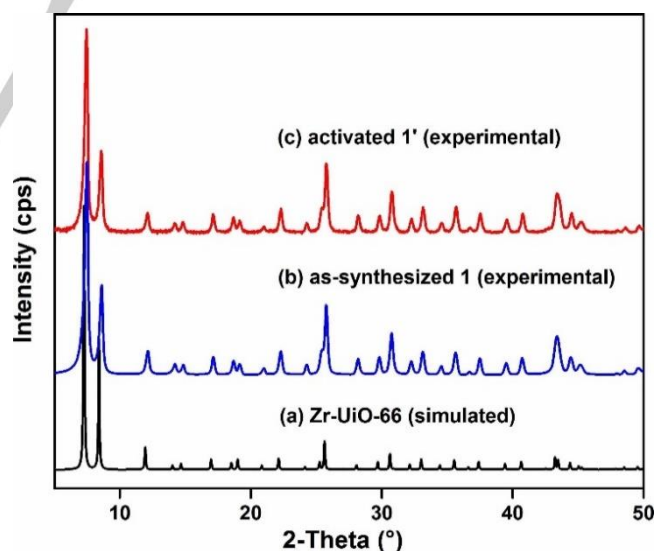


Figure 1. XRPD patterns of (a) Zr-UiO-66 (simulated), (b) as-synthesized **1** (experimental) and (c) activated **1'** (experimental).

XRPD analysis

The XRPD patterns of compound **1** and compound **1'** were recorded, which are shown in Figure 1. From Figure 1, it is concluded that as-prepared compound **1** has similar XRPD pattern as UiO-66 MOF in terms of peak position and peak

intensity. Hence, **1** has same framework topology as the parent UiO-66 MOF.^{18, 53} From Figure 1, it is also concluded that **1** is stable enough under the activation conditions and it has preserved the UiO-66 framework topology even after being converted to **1'**.^{18, 51, 53} To determine the unit cell parameters, the indexing of the XRPD pattern of **1** was performed. The unit cell parameters (SI, Table S1) confirm that the framework of **1** has UiO-66 topology.⁵³ Furthermore, the Pawley refinement of XRPD pattern of **1** was carried out. The result obtained from Pawley fit (SI, Figure S5) is in good agreement with the simulated XRPD pattern of Zr-UiO-66 MOF. Hence, these results also verify that **1** has UiO-66 framework topology.⁵³

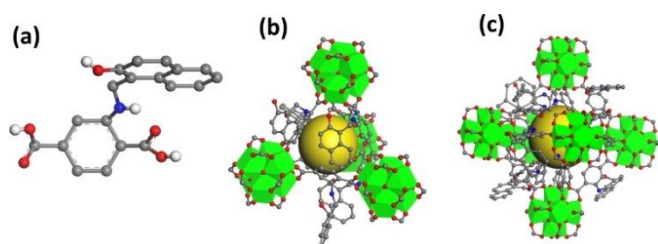


Figure 2. Ball-and-stick representation of (a) H₂BDC-NH-CH₂-Naph-OH linker, (b) tetrahedral and (c) octahedral cages present within the framework structure of **1**. Color codes: Zr, green polyhedra; C, gray; O, red; N, blue; H, white. The cavities are represented by yellow spheres. The structure of **1** was modeled and drawn by using the Materials Studio (version 5.0, Accelrys Inc., San Diego, 2009) software package.

Structure description

For the structural characterization of material **1**, the XRPD pattern of **1** was compared with the parent UiO-66 MOF (Figure 1). The XRPD data is well matched with the parent UiO-66 MOF in terms of peak positions and peak intensities. In addition, the indexing of XRPD pattern of material **1** was also performed to evaluate the unit cell parameters (SI, Table S1). It was observed that the unit cell parameters obtained after indexing the XRPD pattern of **1** are very similar as the pristine UiO-66 MOF. Furthermore, the Pawley fit of XRPD pattern of **1** was carried out, as shown in (SI, Figure S5). From this Figure, it can be observed that the XRPD pattern of **1** is nicely matched with the XRPD pattern of parent UiO-66 MOF. The observed values of R_{wp} and R_p obtained from the Pawley fit are 5.18 and 3.79, respectively. All these data corroborate that the framework of **1** is isostructural with UiO-66. Hence, the framework of **1** contains [Zr₆O₄(OH)₄]¹²⁺ clusters as secondary building units (SBUs) and these SBUs are interconnected with the carboxylate ends of H₂BDC-NH-CH₂-Naph-OH linker. From Figure 2, it can be seen that the framework of **1** has both octahedral as well as tetrahedral cages. Each zirconium atom resides in a square antiprismatic coordination environment.

Thermal stability

Thermal stability of a MOF is one of the crucial issues in determining its applications. Hence, the thermal stability of **1'** was investigated. For the study of thermal stability of MOF in the solid phase, the sample was placed in a thermogravimetric analyzer and heated up from 25 to 700 °C at a constant heating rate of 10 °C/min in argon atmosphere. From (SI, Figure S6), it is inferred that both **1** and **1'** are stable up to 285 °C. The thermal stability of compound **1** and **1'** is comparable with existing UiO-66 type MOFs.^{18, 54}

From (SI, Figure S6), it is observed the thermal treatment of **1** caused three weight loss steps. The first weight loss (2.4 wt%) occurred in the temperature range of 25-160 °C (calcd.: 2.3 wt%) due to the loss of four water molecules. The second weight loss was found to be 10.4 wt% due to the loss of 4.5 DMF molecules (calcd.: 10.6 wt%). The linker molecules start to be eliminated from the framework of **1** beyond 285 °C. Therefore, it is confirmed that **1** is stable up to 285 °C.

Chemical stability

To investigate the chemical stability of coordination bonds inside the framework of MOF, material **1'** was immersed in water as well as acidic (glacial acetic acid and 1 M HCl) and basic (0.1 M NaOH) media. Material **1'** was stirred in these four solvent systems for 10 h at room temperature. Afterward, the solid powder was collected by vacuum filtration and dried at 80 °C inside an oven. After drying, the XRPD patterns of these powder materials were recorded. Figure S7 discloses high stability of material **1'** in aqueous and acidic conditions. It is noteworthy that material **1'** showed instability in a basic medium (0.1 M NaOH, Figure S7). Hence, it is concluded that material **1'** shows high chemical stability like the previously reported, analogous UiO-66 MOF systems.^{18, 55}

N₂ sorption analysis

To determine the BET surface area and nature of porosity, N₂ sorption experiment was carried out with **1'** at -196 °C. Upon N₂ sorption measurement, the specific BET surface area was found to be 946 m² g⁻¹. The micropore volume at $p/p_0 = 0.5$ corresponded to 0.51 cm³ g⁻¹. Remarkably, the observed surface area is high in spite of having a large functional moiety in the side chain of the linker molecule. The typical BET surface area of un-functionalized Zr-UiO-66 MOF falls in the range of 850-1050 m² g⁻¹.^{56, 57} But, **1'** has a BET surface area of 946 m² g⁻¹ in spite of having large side chain attached with the parent linker (BDC) molecule. This type of high BET surface area is generally observed due to the presence of 'missing linker defects/missing cluster defects' inside the MOF framework.⁵⁸⁻⁶⁰ The N₂ sorption curve reveals microporous nature of the compound (SI, Figure S8). The BET surface area as well as micropore volume are in good agreement with the reported UiO-66 MOF.^{54, 61, 62} The pore size distribution curve is displayed in (SI, Figure S9), which shows that the micropores of **1'** are centered at 15.4 Å.

CATALYTIC STUDIES

Study of catalytic activity

The catalytic activity of **1'** was studied in the ring-opening reaction of the of styrene oxide by methanol to obtain 2-methoxy-2-phenylethanol as the only product. The reaction was optimized in terms of catalyst loading and temperature. A blank test in the absence of catalyst showed around 10% conversion of styrene oxide in methanol at 60 °C while 96% conversion was achieved with **1'** as a catalyst in methanol at 60 °C. The time conversion plot for the ring-opening of styrene oxide in methanol with **1'** as a catalyst is shown in Figure 3. Further, the effect of catalyst loading for the ring-opening of epoxide was performed at three catalyst dosages and the observed results are given in Figure 4. These results indicate that the conversion of styrene oxide effectively enhanced upon increasing the catalyst dosage from 3 to 6 mg and a further increase in catalyst loading affords

the quantitative conversion of styrene oxide. On the other hand, a similar trend was observed in the effect of temperature. The conversion of styrene oxide was gradually increased upon increasing the reaction temperature from room temperature to 50 °C and the maximum conversion was attained at 60 °C. The observed catalytic data are presented in Figure 5.

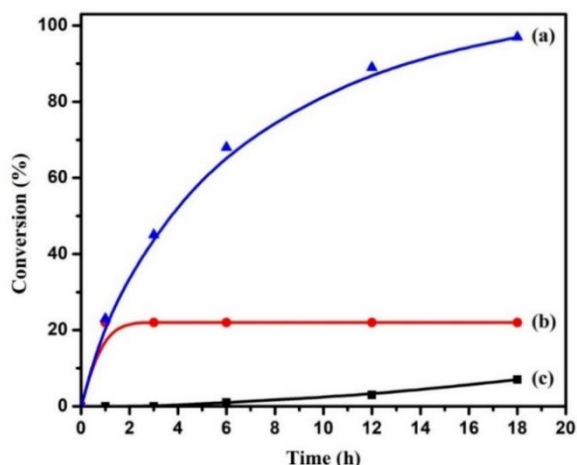


Figure 3. Time conversion plots for the methanolysis of styrene oxide (a) in the presence of **1'**, (b) hot filtration test and (c) blank control experiment.

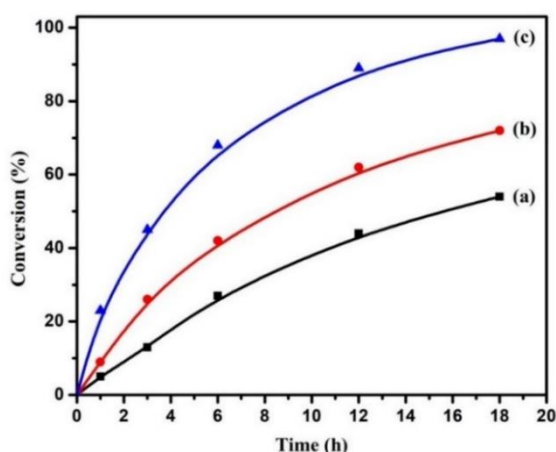


Figure 4. Effect of catalyst loading for the methanolysis of styrene oxide (a) 3 mg, (b) 6 mg and (c) 10 mg of **1'**.

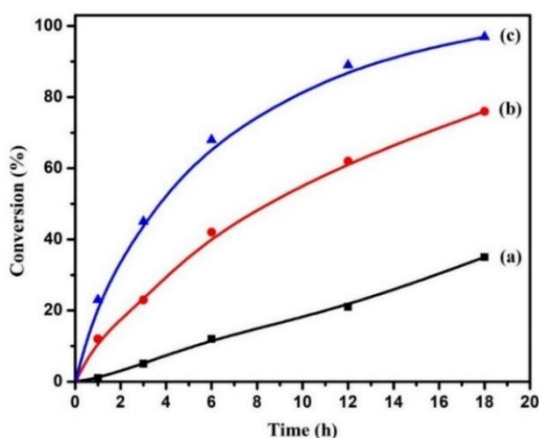


Figure 5. Effect of temperature for the methanolysis of styrene oxide: (a) room temperature (b) 50 °C and (c) 60 °C using **1'** as solid catalyst.

Comparative catalytic study and reaction mechanism

In order to gain an understanding of reaction mechanism in the methanolysis of styrene oxide using **1'** as solid catalyst under the present reaction conditions, the activity of **1'** was compared with UiO-66(Zr) and the linker ($\text{H}_2\text{BDC-NH-CH}_2\text{-Naph-OH}$). The catalytic performance of **1'** was compared with UiO-66(Zr) and **1** (Figure S10, Supporting Information). The observed results clearly suggest that **1'** shows a two-fold enhanced activity than UiO-66(Zr) catalyst and higher activity than pristine **1**. This superior behavior of **1'** than UiO-66(Zr) and **1** is due to the existence of dual active sites like LA and HBD sites.²⁴ The LA originates from metal centers while the HBD sites arise due to the availability of OH and NH groups in the linker. The lower activity of UiO-66(Zr) is due to the lack of these HBD sites. The notable difference in the catalytic behavior between **1** and **1'** (SI, Figure S10) suggest the crucial role of activation in removing the loosely bound solvent molecules by lowering the diffusion limitation to reach the active sites. This hypothesis was confirmed by performing an additional control experiment with the linker ($\text{H}_2\text{BDC-NH-CH}_2\text{-Naph-OH}$). The conversion of styrene oxide with $\text{H}_2\text{BDC-NH-CH}_2\text{-Naph-OH}$ linker as homogeneous catalyst was almost identical to **1'**, but with higher initial activity. This enhanced initial activity shown by the linker is due to the availability of HBD sites which can readily interact with oxygen of styrene oxide through weak hydrogen bond interactions and these sites are readily accessible than **1'**. On the other hand, the use of ZrCl_4 as a homogeneous solid catalyst afforded the desired product in 97% conversion after 1 h under identical conditions. This superior activity is due to the inherent Lewis acidity and efficient interaction of styrene oxide with Zr(IV) sites without experiencing diffusion limitation. Further, pyridine was used as a catalyst poison to quench the active sites in UiO-66(Zr), $\text{H}_2\text{BDC-NH-CH}_2\text{-Naph-OH}$ linker and **1'**. The observed results are shown in Figure 6. The catalytic data with and without pyridine for all these catalysts clearly indicate that pyridine interacts strongly with the LA/HBD sites, thus exhibiting a long induction period (6 h) while it is absent in the absence of pyridine. These catalytic data confirm that pyridine strongly inhibits the interaction of styrene oxide with these active sites. Furthermore, the interaction of styrene oxide with the LA/HBD sites activates the adjacent carbon for nucleophilic attack as shown in Scheme 1b.

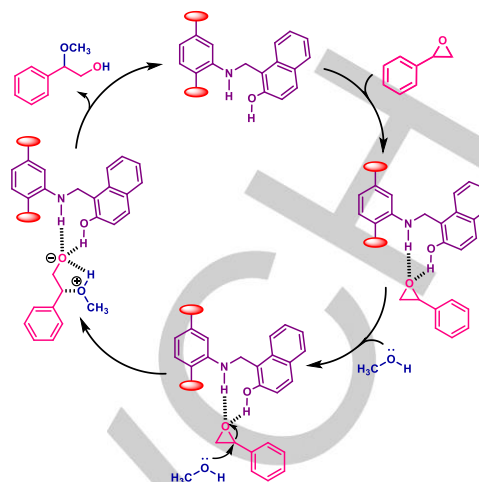
The ring-opening of styrene oxide by methanol using **1'** as catalyst required 18 h at 60 °C. The activity of **1'** was compared with other reported catalysts like Fe(BTC) and $\text{Cu}_3(\text{BTC})_2$ under identical conditions. Styrene oxide conversion was 98% after 12 h using Fe(BTC) while $\text{Cu}_3(\text{BTC})_2$ exhibited 90% conversion after 1 h. These results are shown in Figure 7. The results suggest that the activity of a solid catalyst mainly depends on the nature and accessibility of active sites. The inherent LA of Cu^{2+} in $\text{Cu}_3(\text{BTC})_2$ favors to reach high conversion of styrene oxide within 1 h without diffusion limitation while Fe(BTC) offers much lower activity due to comparatively lower LA sites. On the other hand, the activity of **1'** is slightly lower with these two catalysts and this may be attributed to the steric crowding caused by the bulky linker. In any case, the active sites are accessible by reactants and **1'** can promote this reaction. These comparative studies indicate that although the activity of **1'** is lower than other MOFs, the study provides sufficient evidences that LA and HBD sites can be distinctly installed in the MOF structures and these sites can be effectively employed for

catalytic reaction. In addition, this work also provides alternative types of active sites like HBD sites than the very often used SO_3H moiety as BA sites for this reaction.

Scheme 2 shows the proposed mechanism for the ring opening of styrene oxide by methanol involving the contribution of HBD sites. The observed catalytic data has shown that the influence of HBD sites are much stronger than LA sites. The presence of NH and OH groups in the linker coordinates with oxygen of styrene oxide by forming weak hydrogen bonds thus decreasing the electron density in the adjacent carbon containing phenyl groups. Thus, methanol readily attacks this carbon to initially form an intermediate which upon hydrogen transfer leads to the final product.

One of the general tendencies in heterogeneous catalysis is to ascertain the heterogeneity of the catalytic reaction. Hence, hot filtration test was performed to ensure the absence of leached active species in the solution from the solid catalyst. This test was performed by filtering the solid after 1 h under the reaction temperature and the resulting reaction mixture was stirred for the remaining period. The time conversion plot (Figure 3) indicates that the reaction is completely inhibited upon removal of catalyst from the reaction, thus suggesting the absence of active sites in the solution. Thus, this test proved the heterogeneity of the reaction. Further, ICP-AES analysis of the reaction mixture indicated the absence of Zr, thus ruling out the possibility of metal leaching.

Performing the reusability test in consecutive cycles is another way to confirm the catalyst stability in heterogeneous catalysis. In this aspect, the reusability of **1'** was performed in the ring-opening of styrene oxide by methanol at 60 °C. After the reaction, the solid was washed with methanol, dried and reused in consecutive cycles with the fresh reactants. The attained catalytic results exhibited in Figure 8 indicate that the catalyst retains its activity up to four cycles with no appreciable decay in its activity. An identical activity was achieved in four consecutive cycles upon repeated uses of **1'**, suggesting that the density of active sites remains unaltered under the present reaction conditions. The structural stability of **1'** was examined by the XRPD study, FT-IR, EDX and FE-SEM analyses. The XRPD study (Figure 9) suggested that catalyst **1'** is structurally stable enough through the catalytic reaction up to four consecutive cycles. The FT-IR spectra of the recovered MOF after the first and fourth catalytic cycle of reaction are shown in Figure S4 (Supporting Information). These spectra clearly reveal that there are peaks at 1572 and 1434 cm^{-1} which are due to the asymmetric and symmetric stretching vibrations of carboxylates bonded with Zr^{4+} inside the MOF catalyst, respectively. The presence of these peaks confirms that the MOF catalyst is stable enough even after the fourth catalytic cycle. Furthermore, EDX studies (SI, Figures S11-S14) showed that the atomic percentage of the elements (C, N, O and Zr) present in **1'** before and after four cycles of catalysis is almost close to each other. In addition, the FE-SEM analyses (SI, Figures S15-S16)) confirmed that catalyst **1'** has similar morphology for fresh and reused (for four cycles) samples.



Scheme 2. A proposed mechanism for the ring opening of styrene oxide by methanol involving HBD sites.

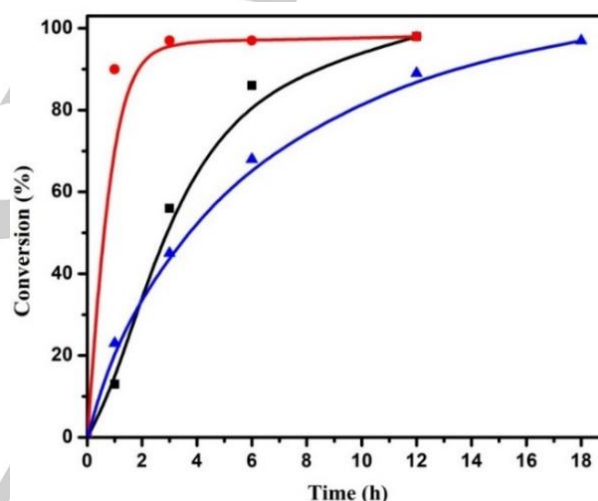


Figure 6. Time conversion plots for the methanolysis of styrene oxide using (●) $\text{H}_2\text{BDC-NH-CH}_2\text{-Naph-OH}$ linker, (▲) **1'**, (■) Zr-Uio-66 and pyridine (0.25 mmol) as catalyst poison with (Δ) Zr-Uio-66-NH-CH₂-Naph-OH, (□) Zr-Uio-66 and (○) $\text{H}_2\text{BDC-NH-CH}_2\text{-Naph-OH}$ linker.

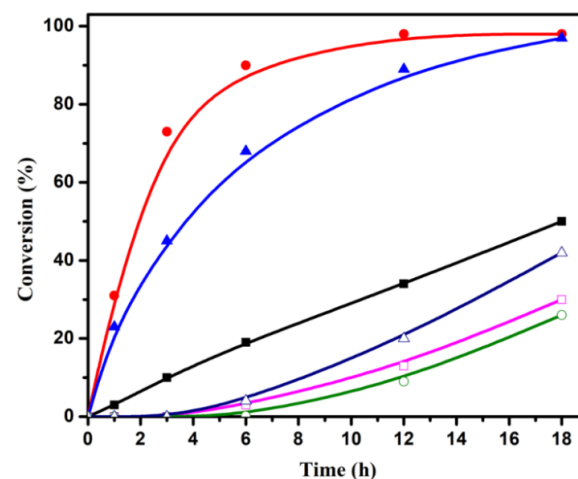


Figure 7. Time conversion plots for methanolysis of styrene oxide by (●) $\text{Cu}_3(\text{BTC})_2$, (■) $\text{Fe}(\text{BTC})$ and (▲) **1'**.

Catalytic studies with various substrates

With the optimized reaction conditions in hand, the scope of **1'** was screened with other epoxides and alcohols, and the observed results are discussed in Table 1. The ring-opening of styrene oxide by methanol using **1'** as solid catalyst afforded 96% conversion after 18 h at 60 °C. Under identical conditions, the conversion of styrene oxide was slightly decreased with ethanol as the nucleophile. Further, the reactivity of styrene oxide with 2-propanol and 1-butanol was further decreased to 78 and 74% conversions, respectively, compared to methanol. This lower conversion of styrene oxide upon the increase of chain length in alcohol is probably due to the lower nucleophilicity and diffusion limitations imposed by the bulkier nature of these alcohols. The observed catalytic data are in good agreement with earlier results in the literature.^{24, 31, 36, 63-65} Interestingly, our hypothesis of the steric hindrance of alcohol was proved by observing distinct reactivity between 1-butanol and *t*-butanol with styrene oxide affording 74 and 35% conversions, respectively, under identical conditions.

On the other hand, the ring-opening reaction between styrene oxide with 1-octanol showed 62% conversion after 18 h, and no further significant change in the conversion was seen even after doubling the reaction time. Ring-opening of styrene oxide by cyclohexanol showed 31% conversion, and this lower activity may be due to the steric hindrance of reactants. On the other hand, ring-opening of cyclohexene oxide by methanol showed a significantly higher conversion of 82% under similar conditions, showing the facile diffusion of these reactants than to the previous case. The enhanced reactivity was observed for 2-methylpropene oxide than to 2-chloromethyloxirane by methanolysis under similar conditions, and this reactivity difference is due to the difference in the diffusion ability of these epoxides to interact with the active sites in **1'**. The later substrate finds more difficulty in reaching the active sites while the former substrate with its smaller dimension can easily penetrate the pores to interact with active sites easily, thus enhancing the electrophilicity in epoxide for methanol attack. These catalytic data clearly confirm that the reaction occurs within the pores of the solid **1'**, thus supporting the size selective catalysis.

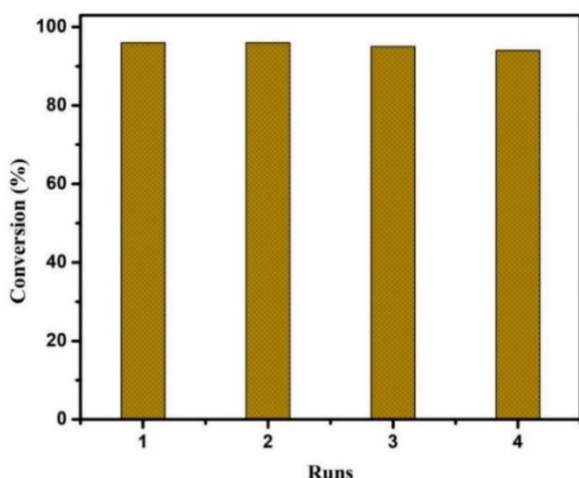


Figure 8. Reusability profile for the methanolysis of styrene oxide using **1'** as a solid catalyst.

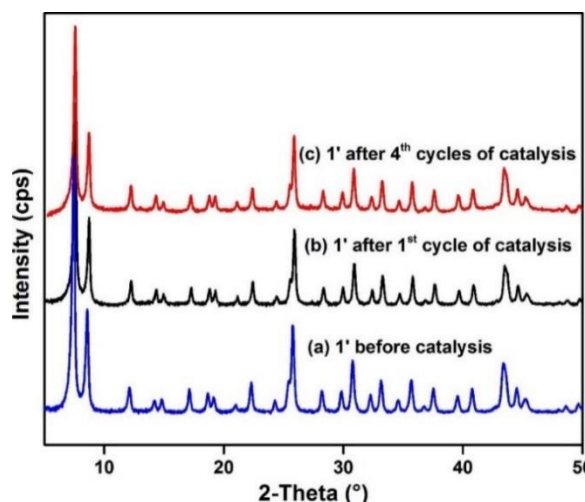
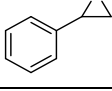
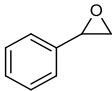
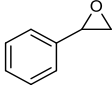
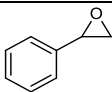
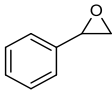
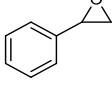
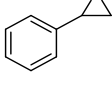
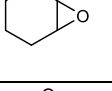
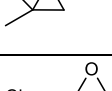
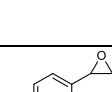
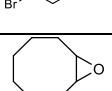
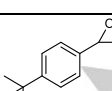
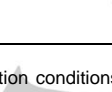


Figure 9. XRPD patterns of **1'** (a) before catalysis, (b) after the 1st cycle and (c) after the 4th cycle of catalysis.

The diffusion limitation exerted by **1'** in the catalytic performance in the opening of epoxide was further verified by conducting additional experiments with epoxies possessing larger kinetic diameters. The observed results are shown in Table 1 and Figures S36-S37 (Supporting Information). 4-Bromostyrene oxide afforded 52% conversion with methanol using **1'** under identical conditions with high regioselectivity of type I isomer. Further, 4-*t*-butylstyrene oxide exhibited trace conversion (3%) while cyclooctene oxide showed no reactivity under identical conditions, thus clearly suggesting the influence of substrate kinetic diameter to diffuse inside the pores of **1'**. On the other hand, the reaction of cyclooctene oxide with methanol in the presence of UiO-66(Zr) afforded around 6% conversion to the desired product with complete selectivity under identical conditions. But, this lower conversion is due to the lack of HBD sites and the nature of cyclic epoxide. These catalytic results prove the size selective catalysis by **1'** and demonstrating the diffusional limitations due to the functionalization of the linker.

Table 1. Alcoholysis of epoxides in the presence of **1'** as hydrogen-bonding organocatalyst.^a

Entry	Epoxide	Alcohol	Time (h)	Conv. ^b (%)	Sel. %	
					Isomer I	Isomer II
1		methanol	18	96	98	2
2		ethanol	18	86	98	2
			24	90	95	5
			95		97	3
3		2-propanol	18	78	94	6
			24	84	94	6
			30	91	96	4
4		1-butanol	18	74	97	3
			24	83	96	4
			36	91	96	4
5		1-butanol	18	35	91	9
			24	41	90	10
			36	51	90	10
6		1-octanol	18	62	97	3
			36	67	97	3
7		cyclohexanol	18	31	94	6
			36	47	92	8
8		methanol	18	82	100	-
			30	98	100	-
9		methanol	18	90	8	92
			30	98	7	93
10		methanol	18	29	100	-
			36	58	98	2
11		methanol	18	52	96	4
12		methanol	18	-	-	-
13		methanol	18	3	97	3

[a] Reaction conditions: epoxide (0.25 mmol), alcohol (2 mL), Zr-Uio-66-NH-CH₂-Naph-OH (10 mg), 60 °C. [b] Conversion and selectivity were determined by GC. Selectivity of isomer I indicates 2-alkoxy-2-phenylethanol and selectivity of isomer II represents other isomers.

Conclusion

To summarize, a new functionalized Zr-Uio-66 MOF with HBD sites in the linker has been developed as a heterogeneous catalyst for the methanolysis of epoxides. We have judiciously designed and successfully synthesized catalyst **1'** by traditional solvothermal method followed by the activation procedure. The catalyst **1'** was characterized by FT-IR, XRPD, TGA, BET, EDX and FE-SEM analyses. The catalytic activity of **1'** was tested in the methanolysis of epoxide with styrene oxide as a model substrate and the activity of catalyst **1'** was also examined with various alcohols. The catalytic reaction was optimized in terms of catalyst loading and temperature. Catalyst **1'** showed 96% conversion of styrene oxide to its corresponding product with 98% regioselectivity. A series of control experiments indicated that catalysis occurs within the pores of **1'** and the participation of dual active sites like LA and HBD sites simultaneously, among which the later sites predominant in the catalytic activity. Catalyst **1'** showed similar catalytic performance in four cycles. A comparison of the fresh and four times used **1'** revealed that the crystalline nature and morphology of the used solids match well with the fresh solid, thus exhibiting high stability under these experimental conditions. Finally, the present catalytic data clearly suggest that the design of this new functionalized MOF possessing HBD sites provides the possibility of developing heterogeneous solid catalyst to mimic the enzyme as well as organocatalysts behavior in MOFs, thus experiencing dual active sites (LA and HBD) within the framework to accelerate the reaction rate in the alcoholysis of epoxide.

Experimental Section

Synthesis of [Zr₆O₄(OH)₄(BDC-C₁₁H₁₀NO)₆]-4H₂O-4.5DMF (Zr-Uio-66-1-(aminomethyl) naphthalen-2-ol, **1**).

ZrCl₄ (28 mg, 0.12 mmol) and 2-(((2-hydroxy naphthalene-1-yl)methyl)amino)terephthalic acid (H₂BDC-C₁₁H₁₀NO) (40 mg, 0.12 mmol) was mixed in 3 mL *N,N*-dimethylformamide (DMF) inside a sealed tube. This reaction mixture was sonicated for 20 min and then 210 µL of acetic acid was added. The total reaction mixture was allowed to heat onto a pre-heated block heater at 120 °C and heating was continued up to 24 h. After 24 h, the tube was cooled to room temperature and the solid precipitation was filtered through membrane filter paper. The powdered material was dried inside an oven at 60 °C for 2 h. The yield was 35 mg (0.011 mmol, 56%) based on zirconium tetrachloride salt. Elem. anal. calcd for C_{127.5}H_{127.5}N_{10.5}O_{46.5}Zr₆ (3098.26 g mol⁻¹): C, 49.43; H, 4.15; N, 4.75%. Found: C, 49.26; H, 4.03; N, 4.51%. FT-IR (KBr, cm⁻¹): 3369 (br), 1656 (vs), 1573 (vs), 1496 (w), 1435 (s), 1385 (s), 1259 (vs), 1157 (w), 1102 (w), 1022 (w), 965 (w), 796 (vs), 767 (vs), 664 (vs), 571 (w), 481 (vs).

Activation of compound **1**

The as-synthesized compound **1** (100 mg) was stirred in 30 mL of methanol for one day. Afterward, the solid was filtered through membrane filter paper and the powder was dried at 70 °C for 2 h. In the next step, this oven-dried powder was activated by heating at 120 °C for one day under vacuum conditions. In this process, the activated compound (**1'**) was achieved.

Reaction procedure for catalysis

A 15 mL oven-dried Schleck tube was charged with **1'** (10 mg) and styrene oxide (0.25 mmol) and HPLC grade methanol (2 mL) was added to this mixture. Then, this heterogeneous slurry was stirred at 60 °C for the required time, as shown in Table and Figures. The conversion of styrene oxide was measured by collecting samples from the reaction mixture at different time intervals. The samples were analyzed in Agilent 7820A gas chromatography (GC) (SI, Figures S17-S37). Conversion and selectivity were determined by the same instrument using the internal standard method. The reusability test was performed for **1'** as follows: at the end of the reaction, the solid catalyst was filtered, washed three times with fresh methanol (3 × 5 mL) and dried at 60 °C for 3 h. The activity of this dried catalyst was examined in the next cycle with fresh styrene oxide and methanol.

Acknowledgements

AD and SB are grateful for financial assistance from Science and Engineering Research Board, New Delhi via grant no. EMR/2016/006500 and EEQ/2016/000012, respectively.

Keywords: Metal-organic framework • UiO-66 • Catalysis • Hydrogen bonding site • Regioselectivity.

References:

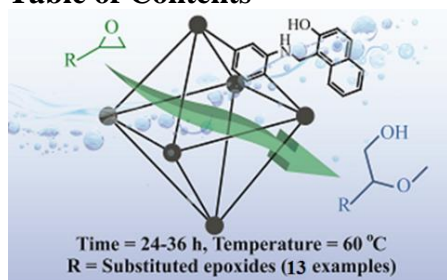
- [1] S. Abednatanzi, P. G. Derakhshandeh, H. Depauw, F.-X. Coudert, H. Vrielinck, P. V. D. Voort, K. Leus, *Chem. Soc. Rev.* **2019**, *48*, 2535–2565.
- [2] O. M. Yaghi, G. Li, H. Li, *Nature*. **1995**, *378*, 703–706.
- [3] Z. Li, X. Xing, D. Meng, Z. Wang, J. Xue, R. Wang, J. Chu, M. Li, Y. Yang, *iScience*. **2019**, *15*, 514–523.
- [4] H. Li, K. Wang, Y. Sun, C. T. Lollar, J. Li, H.-C. Zhou, *Mater. Today*. **2018**, *21*, 108–121.
- [5] W. Huang, J. Jiang, D. Wu, J. Xu, B. Xue, A. M. Kirillov, *Inorg. Chem. Commun.* **2015**, *54*, 10524–10526.
- [6] X.-D. Zhu, K. Zhang, Y. Wang, W.-W. Long, R.-J. Sa, T.-F. Liu, J. Lü, *Inorg. Chem.* **2018**, *57*, 1060–1065.
- [7] H. Meng, C. Zhao, M. Nie, C. Wang, T. Wang, *ACS Appl. Mater. Interfaces*. **2018**, *10*, 32607–32612.
- [8] D.-Y. Ma, Z. Li, J.-X. Xiao, R. Deng, P.-F. Lin, R.-Q. Chen, Y.-Q. Liang, H.-F. Guo, B. Liu, J.-Q. Liu, *Inorg. Chem.* **2015**, *54*, 6719–6726.
- [9] R. Ricco, W. Liang, S. Li, J. J. Gassensmith, F. Caruso, C. Doonan, P. Falcaro, *ACS Nano*. **2018**, *12*, 13–23.
- [10] V. Stavila, A. A. Talina, M. D. Allendorf, *Chem. Soc. Rev.* **2014**, *43*, 5994–6010.
- [11] A. Herbst, A. Khutia, C. Janiak, *Inorg. Chem.* **2014**, *53*, 7319–7333.
- [12] F. Chen, K. Shen, J. Chen, X. Yang, J. Cui, Y. Li, *ACS Cent Sci.* **2019**, *5*, 176–185.
- [13] A. Das, N. Anbu, A. Dhakshinamoorthy, S. Biswas, *Microporous Mesoporous Mater.* **2019**, *284*, 459–467.
- [14] K. Berijani, A. Morsali, *J. Catal.* **2019**, *378*, 28–35.
- [15] A. Das, N. Anbu, M. SK, A. Dhakshinamoorthy, S. Biswas, *Inorg. Chem.* **2019**, *58*, 5163–5172.
- [16] T. C. Wang, W. Bury, D. A. Gomez-Gualdro, N. A. Vermeulen, J. E. Mondloch, P. Deria, K. Zhang, P. Z. Moghadam, A. A. Sarjeant, R. Q. Snurr, J. F. Stoddart, J. T. Hupp, O. K. Farha, *J. Am. Chem. Soc.* **2015**, *137*, 3585–3591.
- [17] O. V. Gutov, W. Bury, D. A. Gomez-Gualdro, V. Krungleviciute, D. Fairen-Jimenez, J. E. Mondloch, A. A. Sarjeant, S. S. Al-Juaid, R. Q. Snurr, J. T. Hupp, T. Yildirim, O. K. Farha, *Chem. Eur. J.* **2014**, *20*, 12389–12393.
- [18] A. Das, S. Das, V. Trivedi, S. Biswas, *Dalton Trans.* **2019**, *48*, 1332–1343.
- [19] W. Liang, H. Chevreau, F. Ragon, P. D. Southon, V. K. Peterson, D. M. D'Alessandro, *CrystEngComm*. **2014**, *14*, 6530–6533.
- [20] M. SK, M. R. U. Z. Khan, A. Das, S. Nandi, V. Trivedi, S. Biswas, *Dalton Trans.* **2019**, *48*, 12615–12621.
- [21] Z. H. a. D. Zhao, *CrystEngComm*. **2017**, *19*, 4066–4081.
- [22] B. Li, K. Leng, Y. Zhang, J. J. Dynes, J. Wang, Y. Hu, D. Ma, Z. Shi, L. Zhu, D. Zhang, Y. Sun, M. Chrzanowski, S. Ma, *J. Am. Chem. Soc.* **2015**, *137*, 4243–4248.
- [23] K. Epp, A. L. Semrau, M. Cokoja, R. A. Fischer, *ChemCatChem*. **2018**, *10*, 3506–3512.
- [24] Y.-X. Zhou, Y.-Z. Chen, Y. Hu, G. Huang, S.-H. Yu, H.-L. Jiang, *Chem. Eur. J.* **2014**, *20*, 14976–14980.
- [25] S. M. Bruno, I. S. Gonçalves, M. Pillinger, C. C. Romão, A. A. Valente, *J. Organomet. Chem.* **2018**, *855*, 12–17.
- [26] R. K. Tak, N. Gupta, M. Kumar, R. I. Kureshy, N. U. H. Khan, E. Suresh, *Eur. J. Org. Chem.* **2018**, *2018*, 5678–5687.
- [27] I. Vilotijevic, T. F. Jamison, *Angew. Chem. Int. Ed.* **2009**, *48*, 5250–5281.
- [28] X. Zhang, M. Wang, C. Zhang, J. Lu, Y. Wang, F. Wang, *RSC Adv.* **2016**, *6*, 70842–70847.
- [29] A. A. Tehrani, S. Abedi, A. Morsali, J. Wang, P. C. Junk, *J. Mater. Chem. A*. **2015**, *3*, 20408–20415.
- [30] J. Barluenga, H. Va'zquez-Villa, A. Ballesteros, J. M. González, *Org. Lett.* **2002**, *4*, 2817–2819.
- [31] T. Weil, M. Kotke, C. M. Kleiner, P. R. Schreiner, *Org. Lett.* **2008**, *10*, 1513–1516.
- [32] G. A. Olah, A. P. Fung, D. Meidar, *Synthesis*. **1981**, *1981*, 280–282.
- [33] S. Das, T. Asefa, *ACS Catal.* **2011**, *1*, 502–510.
- [34] M. Gharib, L. Esrafil, A. Morsali, P. Retailleau, *Dalton Trans.* **2019**, *48*, 8803–8814.
- [35] L. H. Wee, F. Bonino, C. Lamberti, S. Bordiga, J. A. Martens, *Green Chem.* **2014**, *16*, 1351–1357.

FULL PAPER

WILEY-VCH

- [36] W. Reeve, I. Christoffel, *J Am Chem Soc.* **1950**, 72, 1480–1483.
- [37] S. H. Lee, E. Y. Lee, D.-W. Yoo, S. J. Hong, J. H. Lee, H. Kwak, Y. M. Lee, J. Kim, C. Kim, J.-K. Lee, *New J. Chem.* **2007**, 31, 1579 – 1582.
- [38] P. J. Deuss, K. Barta, J. G. d. Vries, *Catal. Sci. Technol.* **2014**, 4, 1174–1196.
- [39] D. L. Burnett, R. Oozeerally, R. Pertiwi, T. W. Chamberlain, N. Cherkasov, G. J. Clarkson, Y. K. Krisnandi, V. Degirmenci, R. I. Walton, *Chem. Commun.* **2019**, 55, 11446–11449.
- [40] J. V. Alegre-Requena, E. Marqués-López, R. P. Herrera, D. D. Díaz, *CrystEngComm.* **2016**, 18, 3985–3995.
- [41] L. Zhang, C. Hu, J. Zhang, L. Cheng, Z. Zhai, J. Chen, W. Ding, W. Hou, *Chem. Commun.* **2013**, 49, 7507–7509.
- [42] N. Deshpande, A. Parulkar, R. Joshi, B. Diep, A. Kulkarni, N. A. Brunelli, *J. Catal.* **2019**, 370, 46–54.
- [43] P. Patel, B. Parmar, R. I. Kureshy, N. U. Khan, E. Suresh, *ChemCatChem.* **2018**, 10, 2401–2408.
- [44] B. Parmar, P. Patel, R. S. Pillai, R. I. Kureshy, N.-U. H. Khan, E. Suresh, *J. Mater. Chem. A.* **2019**, 7, 884–2894.
- [45] R. Rink, J. Kingma, J. H. L. Spelberg, D. B. Janssen, *Biochem.* **2000**, 39, 5600–5613.
- [46] M. S. Sigman, E. N. Jacobsen, *J. Am. Chem. Soc.* **1998**, 120, 4901–4902.
- [47] P. R. Schreiner, A. Wittkopp, *Org. Lett.* **2002**, 4, 217–220.
- [48] D. P. Curran, L. H. Kuo, *J. Org. Chem.* **1994**, 59, 3259–3261.
- [49] J. Hine, S. M. Linden, V. M. Kanagasabapathy, *J. Am. Chem. Soc.* **1985**, 107, 1082–1083.
- [50] S. Biswas, P. V. D. Voort, *Eur. J. Inorg. Chem.* **2013**, 2013, 2154–2160.
- [51] M. SK, S. Banesh, V. Trivedi, S. Biswas, *Inorg. Chem.* **2018**, 57, 14574–14581.
- [52] C. Gogoi, H. Reinsch, S. Biswas, *CrystEngComm.* **2019**.
- [53] J. H. Cavka, S. Jakobsen, U. Olsbye, N. Guillou, C. Lamberti, S. Bordiga, K. P. Lillerud, *J. Am. Chem. Soc.* **2008**, 130, 13850–13851.
- [54] S. Nandi, S. Banesh, V. Trivedi, S. Biswas, *Analyst.* **2018**, 143, 1482–1491.
- [55] A. J. Howarth, Y. Liu, P. Li, Z. Li, T. C. Wang, J. T. Hupp, O. K. Farha, *Nat. Rev. Mater.* **2016**, 1, 1–15.
- [56] K. Užarević, T. C. Wang, S.-Y. Moon, A. M. Fidelli, J. T. Hupp, O. K. Farha, T. Frišćić, *Chem. Commun.* **2016**, 52, 2133–2136.
- [57] Z. Su, Y.-R. Miao, G. Zhang, J. T. Miller, K. S. Suslick, *Chem. Sci.* **2017**, 8, 8004–8011.
- [58] H. Wu, Y. S. Chua, V. Krungleviciute, M. Tyagi, P. Chen, T. Yildirim, W. Zhou, *J. Am. Chem. Soc.* **2013**, 135, 10525–10532.
- [59] P. Ghosh, Y. J. Colón, R. Q. Snurr, *Chem. Commun.* **2014**, 50, 11329–11331.
- [60] Y. Jiao, Y. Liu, G. Zhu, J. T. Hungerford, S. Bhattacharyya, R. P. Lively, D. S. Sholl, K. S. Walton, *J. Phys. Chem. C.* **2017**, 121, 23471–23479.
- [61] M. J. Katz, Z. J. Brown, Y. J. Colón, P. W. Siu, K. A. Scheidt, R. Q. Snurr, J. T. Hupp, O. K. Farha, *Chem. Commun.* **2013**, 49, 9449–9451.
- [62] S. J. Garibay, S. M. Cohen, *Chem. Commun.* **2010**, 46, 7700–7702.
- [63] A. Tarlani, M. Joharian, K. Narimani, J. Muzart, M. Fallah, *J. Solid State Chem.* **2013**, 203, 255–259.
- [64] L. Zhang, C. Hu, W. Mei, J. Zhang, L. Cheng, N. Xue, W. Ding, J. Chen, W. Hou, *Appl. Surf. Sci.* **2015**, 357, 1951–1957.
- [65] S. M. Bruno, I. S. Gonçalves, M. Pillinger, C. C. Romão, A. A. Valente, *J. Organomet. Chem.* **2018**, 855, 12–17.

Table of Contents



A reusable Zr(IV)-based UiO-66 MOF was synthesized by employing 1-(aminomethyl)naphthalene-2-ol appended terephthalate linker and Zr(IV) salt via solvothermal method. The catalytic performance of the activated MOF was examined in the ring opening of epoxides by methanol. The observed experimental catalytic data indicated that the superior activity of activated MOF compared to as-synthesized MOF and UiO-66(Zr) is due to the presence of dual active sites comprising Lewis and hydrogen bond donating sites.